SLAC – PUB – 4247
February 1987
(A)

PROGRESS REPORT ON NEW RF BREAKDOWN STUDIES IN AN S-BAND STRUCTURE AT SLAC*

J. W. WANG AND G. A. LOEW

Stanford Linear Accelerator Center
Stanford University, Stanford, California 94305

1. Summary

This paper gives a progress report on RF breakdown studies carried out at SLAC on an S-band standing-wave disk-loaded accelerator structure. The structure is the same as described at two earlier conferences[1,2] but it has been equipped with eight new radial probes and one output port to observe the emission of light, which has not yet been used. The earlier breakdown limit of 144 MV/m equivalent traveling-wave accelerating gradient and 312 MV/m peak surface field has been reached again and possibly exceeded slightly even though the disk iris edges are severely pitted from earlier tests. Using the new probes it has become possible to monitor field emission as a function of azimuthal direction as well as to record the signals generated at the instant of breakdown. Results are given together with some information on the condition of the structure, chemical cleaning and RF processing. The paper ends with the presentation of some speculations and future plans.

2. Consolidation of Results

Earlier[1,2] and recent results for S-band, and C- and X-band[3] tests are summarized in Table 1. The S-band tests were all done with the standing-wave structure shown in Fig. 1 and a 40 MW klystron. The C- and X-band tests were done with single half-cavities and pulsed magnetrons. For the S-band tests, the variation of breakdown as a function of pulse length was studied from 2.5 down to 1.5 μsec with only a 5% increase in gradient at the shorter pulse.

The results in Table 1 scale roughly as $190[f(\mathrm{GHz})]^{1/2}$. Although the functional dependence is the same as predicted by the Kilpatrick criterion, the factor of 190 is roughly 7.5 times higher. Note that this is not surprising since Kilpatrick's theory was originally derived for ions between parallel electrodes and cannot be applicable in its existing form to electrons.

Table 1. Experimentally obtained gradients.

	S-band	C-band	X-band
Frequency (MHz)	2856	4998	9303
Peak surface field (MV/m)	312	445	572
Corresponding traveling-wave accelerating field*	144	205	267
Peak power input (MW)	~37	0.8	1.2
Measured Q	13790	5400	4820
Filling time for critical coupling (μsec)	0.768	0.172	0.082
Pulse length (μsec)	1.5-2.5	3.5	3.8

*Assuming SLAC structure in which $E_S/E_{ACC} = 2.17$.

3. Condition of the S-band Resonant Structure and RF Processing

After the 1986 tests, the S-band structure was let up to air, the end-plates were removed and the cavities were inspected with a borescope. Several of the disk iris edges were found to be pitted and damaged, particularly the disks belonging to the two high-field cavities (the third and sixth cavity from the input end). Also, three or four of the disk edges toward the output end were still covered with a thin coat of stainless steel from an early accident in which an RF focused field-emitted beam had punctured a stainless steel end-plate, causing it to implode and vaporize some of the material inside. Following inspection, eight holes were drilled into the section to install lateral probes, after which the section was chemically cleaned according to the procedure outlined in Table 2.

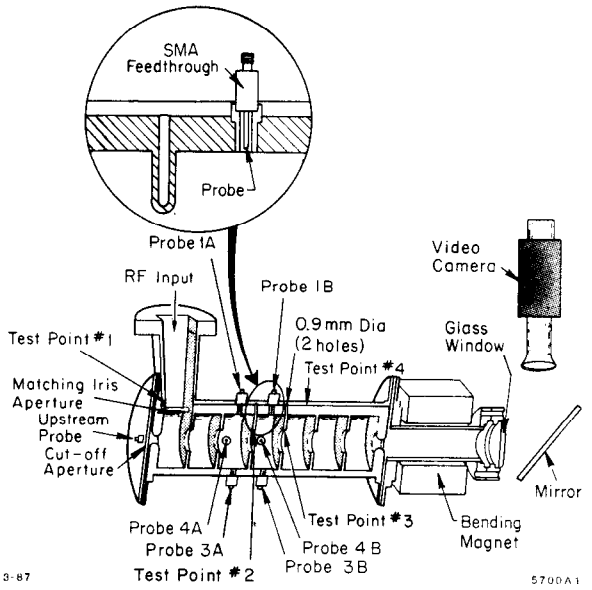

Fig. 1. S-band standing-wave structure. Cavities (A) and (B) are equipped with radial probes. There is also a probe in the cut-off aperture in the input end. The test points are equipped with thermocouples to monitor temperature.

Table 2. Procedure for chemical cleaning.

- Vapor degrease in trichloroethane (5 min.)
- Tap water rinse
- Remove oxide by immersion in non-etch (citrate, McDermid 9268) copper cleaner
- Immerse in potassium cyanide solution (15 sec.)
- Rinse in tap water, cold and hot de-ionized water
- Immerse in 115°F isopropyl alcohol (15 sec.)
- Blow dry with N_2
- Dry in hot air oven at 150°F for two hours

This treatment improved the internal aspect of the cavities considerably but it did not remove the pits nor the stainless steel from the disks. Eight SMA coaxial probes were then brazed into the holes and an optical viewing port was installed (see Fig. 1). In the course of all these procedures, the section was accidentally detuned slightly and it had to be retuned and rematched for critical coupling. Following this, it was rinsed once more with alcohol, dried and installed for RF operation in our heavily shielded vault, and pumped down. RF processing proceeded according to the schedule shown in Fig. 2 without prior *in situ* bake at 250° C as had been used for earlier tests. The entire procedure from 3 MW input power (beginning of arcing) to ~37 MW took approximately 14 hours of running time, with a few major interruptions when the pressure rose to $\sim 10^{-6}$ Torr and was allowed to pump down overnight to $\sim 5 \times 10^{-8}$ Torr.

At this point, it might be useful to describe the RF processing procedure in some detail. RF processing is believed to produce four effects:

a) Removal of adsorbed gas,
b) Removal of dielectric impurities on the surface,
c) Burning of whiskers or microprotrusions, and
d) Smoothing of surface roughness, pits and mountains.

*Work supported by the Department of Energy, contract DE-AC03-76SF00515.

Presented at the 1987 Particle Accelerator Conference, Washington, D.C., March 16–19, 1987

It proceeds most effectively if one raises the RF power level until some breakdown takes place and one then maintains this level until field emission as observed at a probe decreases somewhat. These two steps are repeated a large number of times until one reaches a maximum field barrier which is hard to overcome.

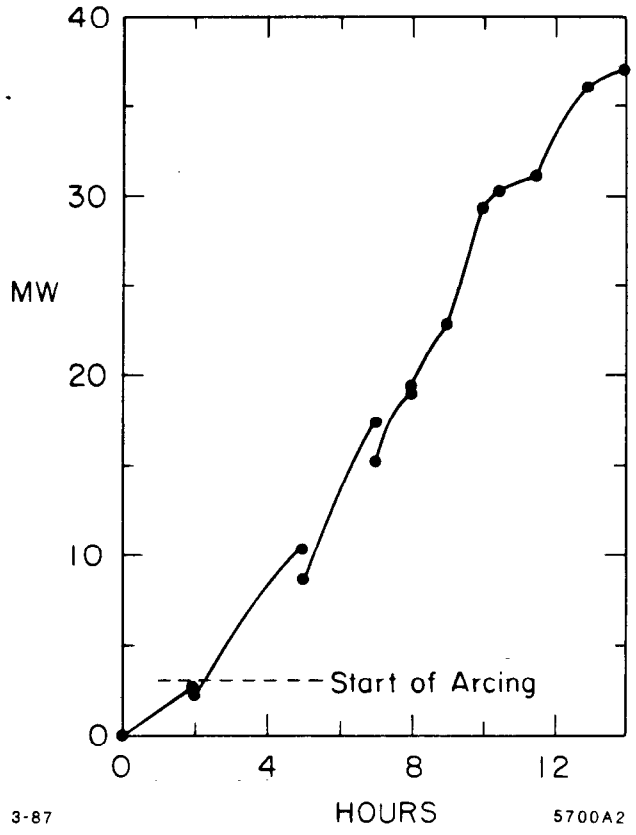

Fig. 2. RF processing schedule.

In this recent experiment, the maximum input power reached was ~ 37 MW which corresponds to a peak field of 312 MV/m, roughly the same as attained during an earlier experiment.

4. Field Emission and Breakdown "Events"

The idea of equipping the third, high-field cavity (A), and the fourth, low-field cavity (B), with four probes at 90° each, was to see if the field emitted current was dominant in any one direction. Labeling probes 1, 2, 3 and 4 clockwise from the top and looking towards the output, we see from the Fowler-Nordheim plots given in Fig. 3 that at the highest field on the left, the first quadrant in cavity (A) exhibited a higher normalized current I_P than the third and fourth quadrants. The currents in cavity (B) were all much lower. The values of I_P were obtained by measuring the voltages V across short coaxial cables of known capacities C in a time t ($I_P \sim CV/t$). The values of the field enhancement parameter β are derived from Fig. 3 by using the expression

$$\frac{d\left(\log_{10} I_P/E_P^{2.5}\right)}{d(1/E_P)} = -\frac{2.84 \times 10^9\, \phi^{1.5}}{\beta} \qquad (1)$$

where ϕ is the work function. Note that the factor 2.84 is roughly half of that (5.8) used in Refs. 1 and 3. The lower value ignores the effect of the so-called retardation of electrons and is used to facilitate comparison with the results of most authors in the field. If the values of β (~60) are ascribed solely to a geometric enhancement at a number of "mountain peaks," the local microscopic field must be approaching 20 GV/m. Other effects such as dielectric enhancement which modify the potential barrier without real field enhancement were probably also present while RF processing was in progress.

Close to the maximum attainable field level, occasional breakdown "events" were observed. A Camac Interface System to a VAX 785 computer was set up to digitize and record eight pulses produced at the instant of breakdown. One such "event" of which more than 80 were recorded is shown in Fig. 4. When a typical breakdown event takes place, predominantly in cavity (A), it is invariably picked up on all four probes in cavity (A), channels 1, 2, 3 and 4, but does not spill over much into cavity (B), channels 5 and 6. Arcing and gasing seem to expand throughout the cavity in all four directions. The seventh channel in Fig. 4 was connected to the probe in the upstream cut-off aperture and the eighth channel to the forward RF pulse. The breakdown current in most recorded events appears after the first microsecond into the pulse, continues for about one microsecond after the end of the pulse while the structure is discharging, and frequently rebounds at a lower level, when the fields have practically died out. The latter phenomenon is not understood but could be due to some form of multipactoring. The current picked up by the probes during breakdown is typically 20 to 40 times greater than the steady-state field-emitted current during pulses preceding the "event." After the "event pulse," breakdown sometimes reappears on a few consecutive pulses as if there were some memory or the original cause persisted, but this effect needs to be studied further.

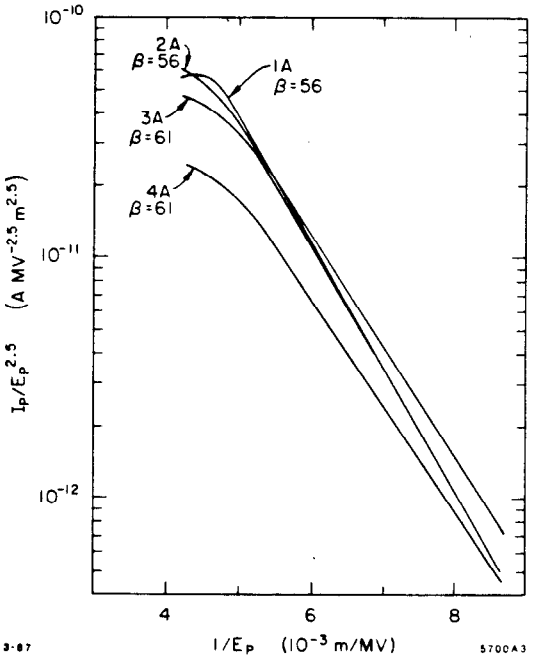

Fig. 3. Field emission current measured at four radial probes in high-field cavity (A).

5. Conclusions, Conjectures and Future Plans

Several interesting conclusions can be drawn from the above results, but several questions also remain unanswered or in doubt, pointing to the need for further work. These are listed below:

1. It is gratifying that the section can still reach the peak surface field of 312 MV/m even though the disks are pitted and damaged.
2. We are still not entirely sure as to which physical phenomenon dominates the onset of the breakdown. We suspect that when the highest surface field (312 MV/m) is approached after several hours of processing, most of the gas and impurities have been driven off the surface, evaporated and pumped away. The breakdown is then

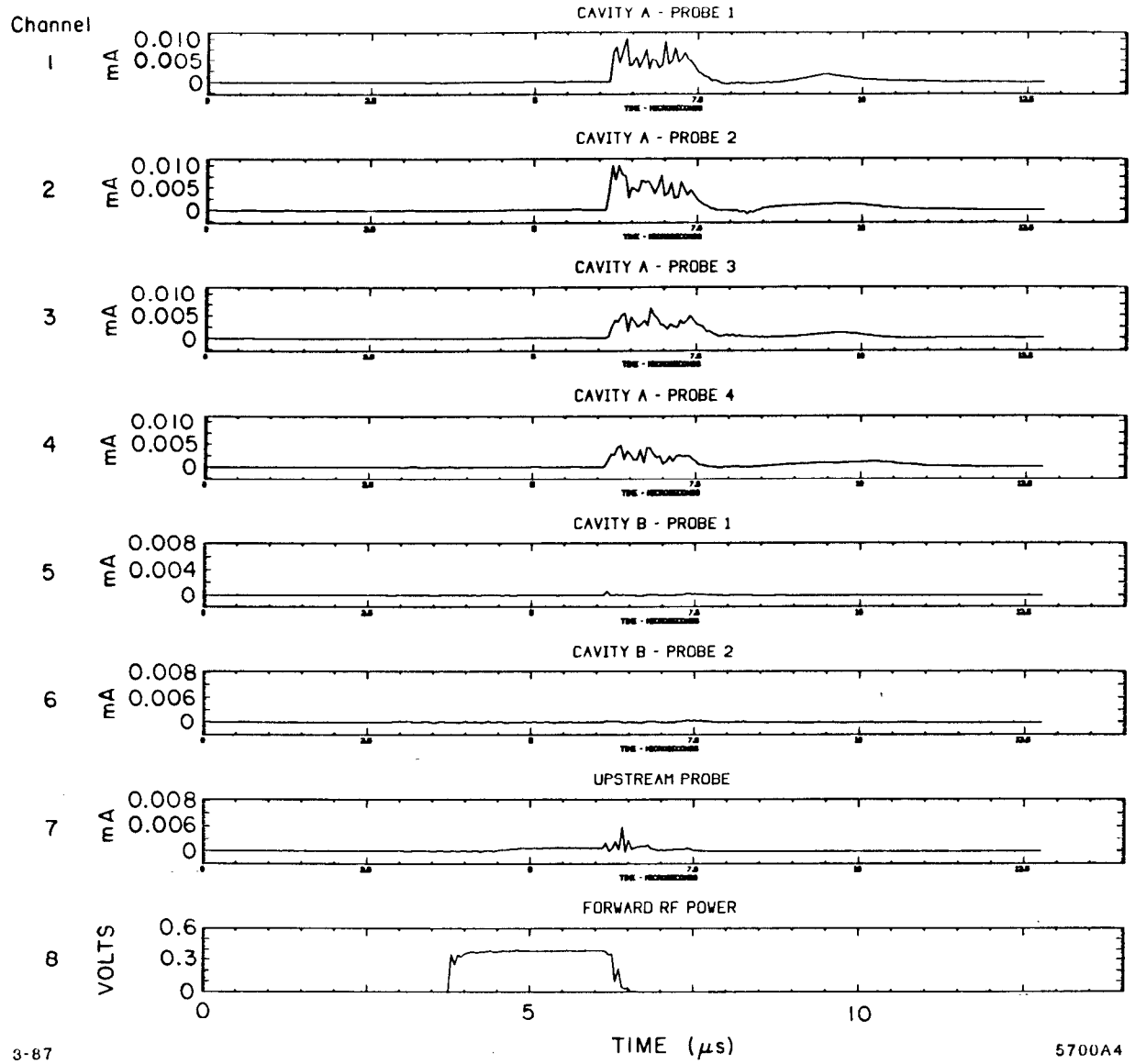

Fig. 4. Breakdown "event" recorded at four radial probes in high-field cavity (A), two radial probes in low-field cavity (B) and one upstream probe. The forward RF pulse provides a time reference.

caused, either at the point of emission by the burn-out of microprotrusions through ohmic loss, or by heating and vaporization of the copper at the point of impact. The resulting puffs of gas become ionized, contributing to the electrons and ions which hit the surfaces and are partially collected by the probes. Given the complexity of the problem, we have not yet been able to derive a theoretical model to predict the $f^{1/2}$ Kilpatrick-like dependence of the breakdown field.

3. It appears that the damage, namely the pits and volcano-like mountains, is produced at the point of impact by the electrons, ions and possibly microparticles. It is not clear what fraction of the RF stored energy in the high-field cavity, approximately 9 Joules, is involved in producing the damage.
4. Given the way in which the RF processing is carried out, namely with the aid of induced breakdown, we wonder whether some of the damage is not inherent in the procedure: i.e., the impact energy which cleans up the surface also produces the effect which ultimately limits the performance at higher fields.
5. Clearly, much more work is needed to elucidate these questions. Some extra information is expected from the observation of light emission which is now possible with the new output ports, but which has not yet been attempted.

Acknowledgements

The authors wish to thank R. H. Miller for helping in retuning and rematching the section, J. M. Zamzow for reinstalling the waveguides and the vacuum system, and P. L. Corredoura for setting up the VAX-785 computer interface system to digitize and record the breakdown pulses.

References

1. RF Breakdown Studies in a SLAC Disk-loaded Structure, by J. W. Wang, V. Nguyen-Tuong and G. A. Loew, Proceedings of the 1986 Linear Accelerator Conference, SLAC-Report-303, September 1986.
2. Measurements of Ultimate Accelerating Gradients in the SLAC Disk-loaded Structure, by J. W. Wang and G. A. Loew, Proceedings of the 1985 Particle Accelerator Conference, Vancouver, B.C., May 1985, SLAC-PUB-3597.
3. Voltage Breakdown at X-band and C-band Frequencies, by E. Tanabe, (Varian Associates, Inc.) J. W. Wang and G. A. Loew (SLAC), Proceedings of the 1986 Linear Accelerator Conference, SLAC-Report-303, September 1986.